IMMUNOLOGY

The catalytic activity of the kinase ZAP-70 mediates basal signaling and negative feedback of the T cell receptor pathway

Hanna Sjölin-Goodfellow,[1,2*†] Maria P. Frushicheva,[3*] Qinqin Ji,[4*] Debra A Cheng,[1,2] Theresa A. Kadlecek,[1,2] Aaron J. Cantor,[5,6] John Kuriyan,[5,6,7,8,9] Arup K. Chakraborty,[3,10,11,12,13,14*‡] Arthur R. Salomon,[4,15*‡] Arthur Weiss[1,2*‡]

T cell activation by antigens binding to the T cell receptor (TCR) must be properly regulated to ensure normal T cell development and effective immune responses to pathogens and transformed cells while avoiding autoimmunity. The Src family kinase Lck and the Syk family kinase ZAP-70 (ζ chain–associated protein kinase of 70 kD) are sequentially activated in response to TCR engagement and serve as critical components of the TCR signaling machinery that leads to T cell activation. We performed a mass spectrometry–based phosphoproteomic study comparing the quantitative differences in the temporal dynamics of phosphorylation in stimulated and unstimulated T cells with or without inhibition of ZAP-70 catalytic activity. The data indicated that the kinase activity of ZAP-70 stimulates negative feedback pathways that target Lck and thereby modulate the phosphorylation patterns of the immunoreceptor tyrosine–based activation motifs (ITAMs) of the CD3 and ζ chain components of the TCR and of signaling molecules downstream of Lck, including ZAP-70. We developed a computational model that provides a mechanistic explanation for the experimental findings on ITAM phosphorylation in wild-type cells, ZAP-70–deficient cells, and cells with inhibited ZAP-70 catalytic activity. This model incorporated negative feedback regulation of Lck activity by the kinase activity of ZAP-70 and predicted the order in which tyrosines in the ITAMs of TCR ζ chains must be phosphorylated to be consistent with the experimental data.

INTRODUCTION

T lymphocytes are a powerful component of our immune defense against microbes and tumor cells; however, if not properly regulated, they can cause severe harm through inflammatory tissue damage during infections and autoimmune reactions. Therefore, precise control mechanisms need to be in place to govern T cell activation. Both T cell development and immune surveillance require the T cell to distinguish and respond appropriately to distinct signals resulting from interactions of the T cell antigen receptor (TCR) with different peptides bound to major histocompatibility complex (MHC) proteins. Antigen recognition by the TCR is interpreted through intracellular signaling events, including phosphorylation of signaling proteins that subsequently determine the proper response. The TCR subunits (the TCRα and β chains, as well as the CD3 γε and δε chains and ζζ subunits) all lack intrinsic kinase activity. Downstream signal transduction relies on the recruitment and activation of protein tyrosine kinases to the CD3 and ζ chains (*1*, *2*).

Signaling is initiated by the Src family kinase Lck, which phosphorylates the two tyrosine residues (Y) in the conserved amino acid sequence D/ExYxxLx(6–8)YxxL, which represents the immunoreceptor tyrosine–based activation motifs (ITAMs) of the TCR CD3 and ζ chains. There are three ITAMs in each ζ chain and one in each of the CD3 chains; hence, the TCR complex contains 10 ITAMs. Doubly phosphorylated ITAMs provide docking sites for the tandem Src homology 2 (SH2) domains of the Syk family kinase ZAP-70 (ζ chain–associated protein kinase of 70 kD). Activated ZAP-70 propagates the signal further downstream, mainly by phosphorylation of the adaptor proteins linker of activated T cells (LAT) and SLP-76 (SH2 domain–containing leukocyte phosphoprotein of 76 kD), which nucleate signaling effector molecules (*1*–*3*).

Lck activity is regulated by its phosphorylation, which mediates conformational changes in Lck as well as its localization (*2*, *4*). Phosphorylation of tyrosine 505 (Tyr^{505}) in Lck by the cytoplasmic tyrosine kinase Csk (C-terminal Src kinase) stabilizes an autoinhibitory conformation that engages the Lck SH2 domain with Tyr^{505} and the SH3 domain with intramolecular proline residues (*4*, *5*). Dephosphorylation of Tyr^{505} is mediated by the receptor-like protein tyrosine phosphatase CD45 (PTPRC). A dynamic steady state regulates the phosphorylation status of this site. The catalytic activity of Lck is promoted by trans-autophosphorylation of the conserved Tyr^{394} on the activation loop of the kinase domain (*2*, *4*, *6*).

[1]Howard Hughes Medical Institute, University of California, San Francisco, San Francisco, CA 94143, USA. [2]Department of Medicine, University of California, San Francisco, San Francisco, CA 94143, USA. [3]Department of Chemical Engineering, Massachusetts Institute of Technology, Cambridge, MA 02142, USA. [4]Department of Chemistry, Brown University, Providence, RI 02912, USA. [5]Department of Molecular and Cell Biology, University of California, Berkeley, Berkeley, CA 94720, USA. [6]California Institute for Quantitative Biosciences, University of California, Berkeley, Berkeley, CA 94720, USA. [7]Department of Chemistry, University of California, Berkeley, Berkeley, CA 94720, USA. [8]Howard Hughes Medical Institute, University of California, Berkeley, Berkeley, CA 94720, USA. [9]Physical Biosciences Division, Lawrence Berkeley National Laboratory, Berkeley, CA 94720, USA. [10]Department of Physics, Massachusetts Institute of Technology, Cambridge, MA 02142, USA. [11]Department of Chemistry, Massachusetts Institute of Technology, Cambridge, MA 02142, USA. [12]Department of Biological Engineering, Massachusetts Institute of Technology, Cambridge, MA 02142, USA. [13]Institute for Medical Engineering & Science, Massachusetts Institute of Technology, Cambridge, MA 02142, USA. [14]Ragon Institute of Massachusetts General Hospital, Massachusetts Institute of Technology, and Harvard University, Cambridge, MA 02139, USA. [15]Department of Molecular Biology, Cell Biology, and Biochemistry, Brown University, Providence, RI 02912, USA.
*These authors contributed equally to this work.
†Present address: Section for Immunology, Department of Experimental Medical Science, Lund University, 22184 Lund, Sweden.
‡Corresponding author. E-mail: as@brown.edu (A.R.S.); arupc@mit.edu (A.K.C.); aweiss@medicine.ucsf.edu (A.W.)

Additional phosphorylation sites contribute to the regulation of Lck, and reports suggest that Lck is present in multiple activation states, even in resting T cells, and that its activity is not changed substantially upon TCR stimulation (*2*, *4*, *7*–*12*).

Activation of ZAP-70 represents a second critical checkpoint in T cell signaling, and several mechanisms operate to ensure tight regulation of this kinase. The current model for the regulation of ZAP-70 includes conformational changes between autoinhibited and activated states. Binding to the doubly phosphorylated ITAMs is believed to initiate the first step in releasing autoinhibition because this step requires repositioning of the SH2 domains in a way that enables their binding to ITAMs but is incompatible with the fully autoinhibited conformation of ZAP-70. The binding event also localizes ZAP-70 at the plasma membrane, where Lck can further promote the active conformation of ZAP-70 by phosphorylation of ZAP-70 Tyr^{315} and Tyr^{319}. Binding of Lck, through its SH2 domain, to the phosphorylated Tyr^{319} ($pTyr^{319}$) of ZAP-70 in turn promotes the activated state of Lck and further facilitates the activation of ZAP-70 through phosphorylation of ZAP-70 on Tyr^{493} in the activation loop (*13*–*16*).

Both positive and negative feedback mechanisms control TCR signaling and the activities of receptor-proximal tyrosine kinases. Tyrosine phosphatases, such as SH2 domain–containing protein tyrosine phosphatase 1 (SHP-1) and protein tyrosine phosphatase, nonreceptor type 22 (PTPN22), reduce the activities of Lck and ZAP-70, thereby dampening or terminating downstream signaling (*2*, *17*–*19*). Other negative regulators include the Csk-interacting adaptor proteins phosphoprotein associated with glycosphingolipid-enriched microdomains (PAG) and Lck interacting transmembrane adaptor 1 (LIME), the E3 ubiquitin ligases c-Cbl and Cbl-b, and docking protein 1 (Dok1) and Dok2, which interact with Csk and Ras guanosine triphosphatase–activating protein (RasGAP) (*20*–*23*). Spatial arrangement of signaling molecules at the T cell immunological synapse (the interface between a T cell and an antigen-presenting cell) also regulates TCR signaling (*24*–*28*); however, the details of these mechanisms and the pathways that connect the different regulatory proteins after TCR ligation still need to be further characterized. In addition, studies support an emerging picture of the basal signaling status in resting T cells as one of a dynamic steady state rather than a silent, fixed state (*7*, *8*, *29*–*31*). In this way, T cells may be poised to very rapidly mount an appropriate response to a stimulus and be able to adjust this resting state according to changes in their surroundings. To prevent T cell activation in the absence of interactions between nonself agonists and the TCR, the ongoing basal signaling should require negative control mechanisms to operate in resting T cells. Studies of TCR signaling regulators such as Csk support this notion, and perturbations of this balance could be involved in the development of autoimmune diseases and immunodeficiencies (*9*, *30*, *32*).

The critical role of ZAP-70 in proper T cell development and T cell function in the periphery is well documented (*33*). Potential negative regulation in the T cell signaling network could involve ZAP-70–mediated control. To characterize potential signaling feedback mechanisms dependent on the catalytic activity of ZAP-70, we used stable isotope labeling by amino acids in cell culture (SILAC) and mass spectrometry–based quantitative phosphoproteomics in combination with rapid inhibition of the catalytic function of ZAP-70. Our results suggest the presence of ZAP-70 kinase–dependent feedback that inhibits both basal signaling and agonist-induced TCR-proximal signaling, targeting ZAP-70 itself as well as the activity of Src family kinases. The data suggest that changes in the phosphorylation of ITAMs in the TCR ζ chains after inhibition of an analog-sensitive mutant of ZAP-70 ($ZAP\text{-}70^{AS}$) differ from previous data obtained from similar methods with ZAP-70 null T cells (*34*). To investigate how a single signaling network can account for this set of observations, we constructed computational models. Our findings suggest that a single signaling module consistent with both sets of data should include ZAP-70–dependent inhibition of Lck activity and one of three possible orders in which the N- and C-terminal tyrosines in the ITAMs are phosphorylated. Future experiments that might discriminate between these possibilities are suggested.

RESULTS

SILAC-based quantitative phosphoproteomic analysis reveals TCR signaling events that depend on the kinase activity of ZAP-70

Our understanding of the mechanisms responsible for feedback and regulation in the TCR signaling network is far from complete. Because ZAP-70 has a key function in TCR signaling, both for the initiation and maintenance of the signal, we hypothesized that its activity might also be needed to properly orchestrate potential feedback mechanisms that regulate signal strength. There is, to date, no selective inhibitor available for the specific targeting of ZAP-70 catalytic activity. Therefore, to reveal feedback pathways dependent on the kinase activity of ZAP-70, we used a genetically selective system in which a bulky analog of the general kinase inhibitor protein phosphatase 1 (PP1) inhibits a mutant of ZAP-70. In this mutant, the gatekeeper Met residue (Met^{414}) is mutated to Ala to create more space in the catalytic site to accommodate a bulky inhibitor. This renders the mutated ZAP-70 susceptible to the bulky analog of PP1, which enables cells that express the wild-type kinase to serve as a control for any off-target effects of the inhibitor. $ZAP\text{-}70^{AS}$ has been introduced in the human Jurkat T cell leukemia cell line p116 (which lacks endogenous ZAP-70) as previously described by Levin *et al.* (*35*). Here, we used a more potent and selective inhibitor, HXJ-42, that we have described and used in studies of thymic development and $CD4^+$ T cell proliferative thresholds in mice expressing the mouse PP1 analog–sensitive mutant of ZAP-70 (*36*, *37*). This system enables the selective inhibition of ZAP-70 kinase activity and efficiently blocks downstream TCR signaling events, such as phosphorylation of the ZAP-70–specific substrates LAT and SLP-76, as well as phosphorylation of downstream signaling molecules, including phospholipase C–γ1 (PLC-γ1) and extracellular signal–regulated kinase (ERK). Our system further enables us to target the catalytic activity of ZAP-70 without compromising its function as an adaptor protein (*38*).

Clues to feedback mechanisms can be obtained by studying fluctuations in intracellular phosphorylation events after the perturbation of signaling pathways. Quantitative mass spectrometry–based technology, such as SILAC, is a powerful tool for studies of large-scale phosphorylation dynamics, and studies have successfully applied this to T cells (*34*, *39*–*41*). By combining this approach with the $ZAP\text{-}70^{AS}$ system, we performed a wide-scale analysis of temporal changes in phosphorylation patterns induced by rapid inhibition of ZAP-70 catalytic activity during basal signaling, as well as after robust TCR stimulation. SILAC-labeled, $ZAP\text{-}70^{AS}$–expressing p116 Jurkat cells were treated with the PP1 analog HXJ-42 (*36*) or dimethyl sulfoxide (DMSO) just before TCR stimulation, and samples were collected at time zero and at three different time points after TCR stimulation (2, 5, and 10 min), with five biological replicates for each condition and time point (Fig. 1 and see Materials and Methods).

We detected, over the time points measured, 905 unique phosphosites on 608 proteins that were quantified by selected ion chromatogram (SIC) peak area integration and statistically analyzed with multiple hypothesis correction (table S1 and S2). We selected some of these peptides (Table 1) on the basis of proteins known to be involved in TCR signaling.

Label-free quantitation
Enables for comparison between multiple time points

Experimental procedure

SILAC quantitation
Enables comparisons between ZAP-70AS cells treated with or without the inhibitor

Cell culture

ZAP-70AS (**light**) ZAP-70AS (**heavy**)

Metabolic labeling
Label cells with light (^{12}C,^{14}N) or heavy (^{13}C,^{15}N) Arg and Lys.

ZAP-70 kinase activity Inhibition

ZAP-70AS (**light**) ZAP-70AS + inhibitor (**heavy**)

Inhibition
Cells labeled with heavy Arg and Lys were treated with inhibitor for 90 s

Stimulation and lysis
Cells are stimulated with anti-CD3 and anti-CD4 antibodies and anti-IgG for 0, 2, 5, or 10 min. Stimulation is halted by lysis.

(0, 2,5, 10) (0, 2,5, 10) (0, 2,5, 10)

Combine
Combine heavy and light lysates at a 1:1 protein ratio

Trypsin digestion

Equal amount of LIEDAEpYTAK peptide is added to each time point before immunoprecipitation.

Tyrosine-phosphorylated peptide enrichment
Phosphotyrosine immunoprecipitation.

Peptide abundance between different time points is normalized to that of an external standard peptide

LC-MS/MS data acquisition
Spectra collected for peptides

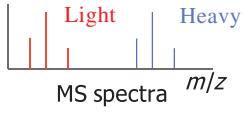

Heavy and light peptides can be distinguished by mass shift created by incorporation of the isotope-labeled amino acids.

Label-free heatmaps generated on the basis of peak area at each time point for each peptide. Black denotes the average peptide abundance. Blue denotes lower than average peptide abundance, whereas yellow denotes higher than average peptide abundance.

Heatmap generation

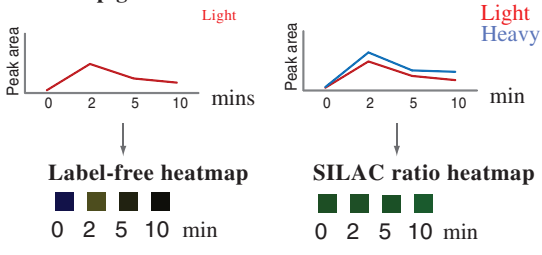

SILAC ratio heatmaps generated on the basis of the ratio of abundance between heavy and light peptides. Black denotes no difference in peptide abundance between heavy and light peptides. Red denotes less abundance of the heavy peptide compared to the light peptide, whereas green denotes the opposite.

Fig. 1. Experimental design for SILAC experiments. Human Jurkat p116 cells expressing ZAP-70AS were incubated with light or heavy stable isotope–labeled arginine and lysine amino acids, physically differentiating the two proteomes by a shift in molecular weight. Cells were treated with DMSO (light-labeled cells) or HXJ-42 (ZAP-70AS + inhibitor, heavy-labeled cells) for 90 s before stimulation. Each cell population was then incubated with OKT3 and OKT4 antibodies against CD3 and CD4, respectively, for 30 s before being treated with cross-linking immunoglobulin G (IgG) for the indicated times. A total of five biological replicates were performed. Sample preparation, mass spectrometry experiments, and data analysis were performed as indicated.

Table 1. SILAC heatmap representation of the temporal changes in the extent of tyrosine phosphorylation of proteins associated with the KEGG (Kyoto Encyclopedia of Genes and Genomes) TCR signaling pathway. Heatmaps were calculated from five independent biological replicate experiments. Green represents enhanced phosphorylation in response to ZAP-70 inhibition, whereas red represents a decrease in the phosphorylation of the indicated proteins relative to that in DMSO-treated control cells. White dots in the heatmap indicate statistically significant differences (Q value < 0.05) for those time points. Below each heatmap square is a color bar representing the percentage confidence value (CV) for the indicated times. PI3K, phosphatidylinositol 3-kinase; RXR-α, retinoid X receptor α; MAPK14, mitogen-activated protein kinase 14.

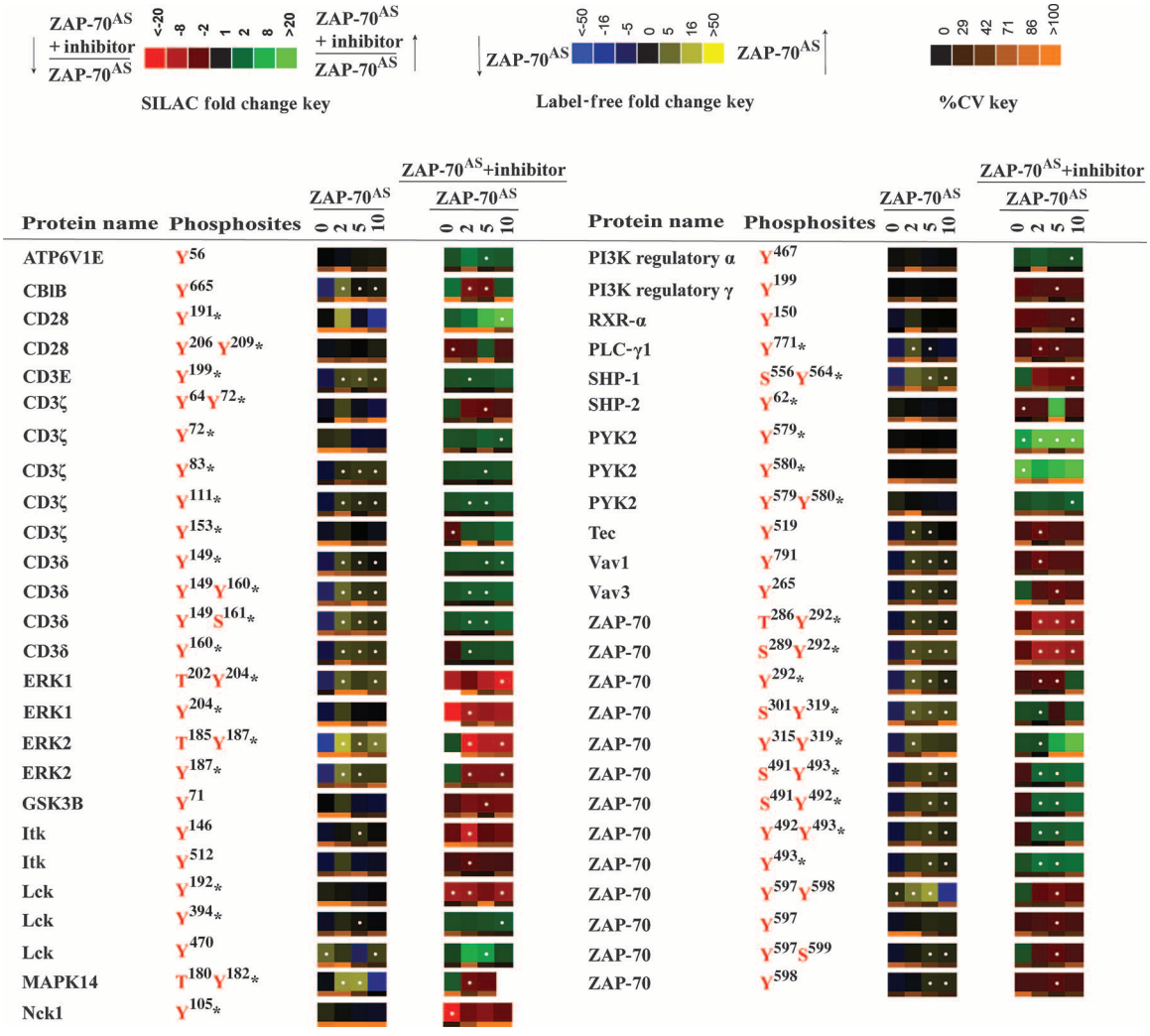

We also calculated the fold change and Q values for these peptides (table S3). A Q value is defined as the measure of the minimum false discovery rate at which a test can be called significant (*42–44*). For each time point, Q values for multiple hypothesis tests were calculated on the basis of the determined P values with the R package QVALUE, as previously described (*42–44*). Label-free data for the control samples in the absence of the inhibitor through a time course of TCR stimulation showed the expected pattern of phosphorylation events associated with TCR signaling. Reproducibility of the SILAC analysis among the replicates was confirmed by evaluating the correlation of $\log_2$-transformed SILAC ratios between each biological replicate in scatter plots (figs. S1 and S2). For each sequenced peptide, quantitative data are represented visually either as a label-free heatmap reflecting changes in abundance over time for each condition in the absence of inhibitor or as a SILAC ratio heatmap reflecting the SILAC ratio for inhibitor-treated ZAP-70AS–expressing cells over the uninhibited control cells.

As expected, inhibition of the catalytic activity of ZAP-70AS resulted in the reduced abundance of downstream phosphorylation events, including a substantial decrease in the phosphorylation of Itk, Vav1, and ERK1/2 (Fig. 2A). However, TCR-induced phosphorylation patterns on receptor-proximal signaling molecules, such as the CD3 chains, the TCR ζ chain, and the kinases Lck and ZAP-70AS, were also altered compared to those of controls (Fig. 2, B and C, and Table 1). In addition, we detected increases and decreases in the abundances of phosphosites of certain signaling molecules in inhibitor-treated cells even before the TCR was stimulated. In particular, statistically significant fold changes (7- to 23-fold) in abundance

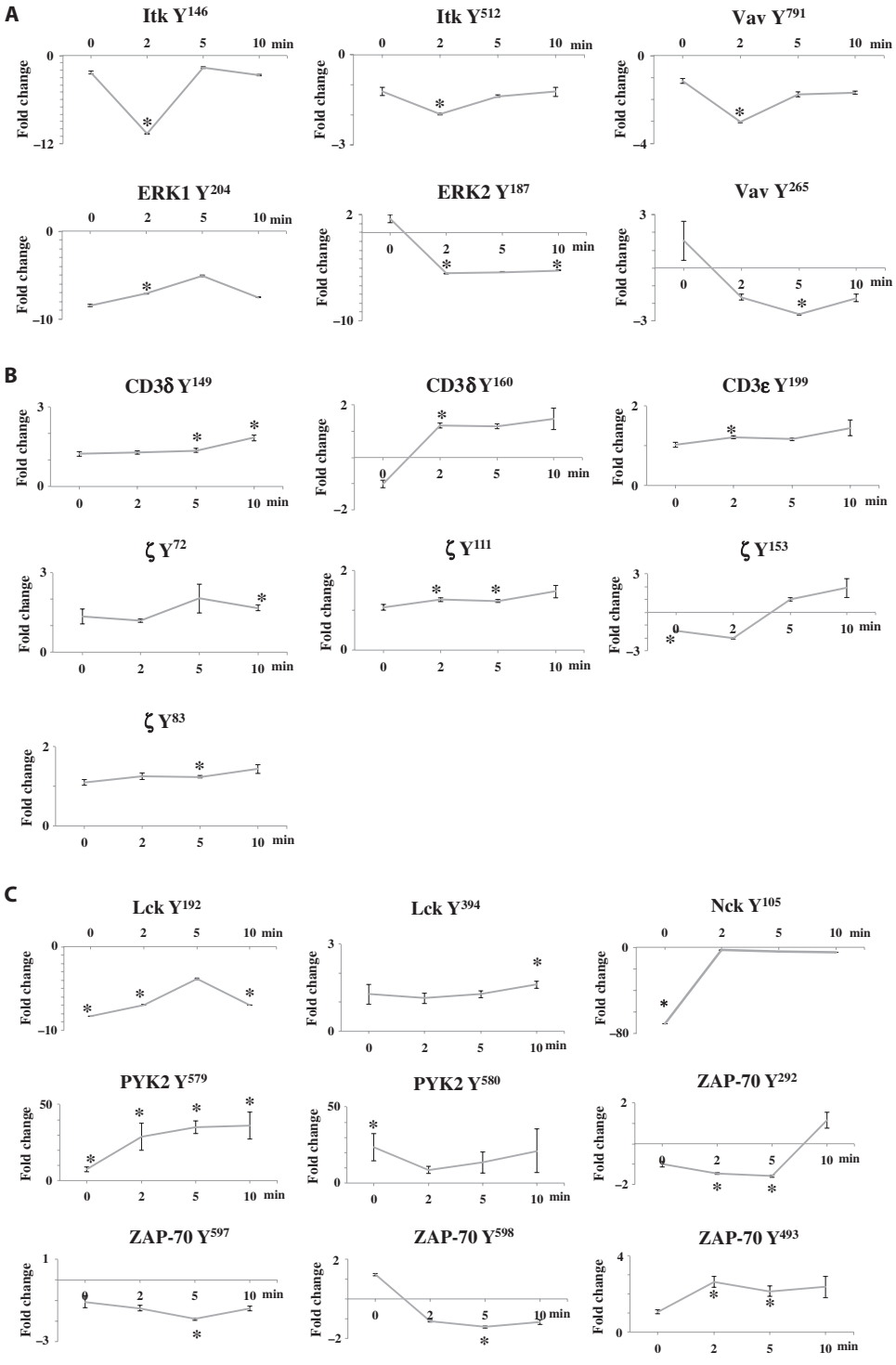

Fig. 2. Individual phosphorylation site changes with inhibitor treatment. (A to C) Comparison of the relative abundances of the indicated phosphopeptides for (A) Itk, Vav, and ERK; (B) CD3 ITAMs; and (C) Lck, ZAP-70, Nck, and PYK2 after cells preincubated with DMSO (control) or the ZAP-70AS inhibitor were left unstimulated (zero time point) or were stimulated through the TCR for the indicated times. A total of five biological replicates were performed, and the calculated average ratio and SD were plotted for each time point. *$P < 0.05$.

were seen in Lck-Tyr^{192}, Nck-Tyr^{105}, Pyk2-Tyr^{579}, and Pyk2-Tyr^{580} after the inhibition of ZAP-70AS (Fig. 2C). We validated the specificity and at least the trend of the changes of some of the phosphosites in both the TCR-stimulated and basal states by performing Western blotting analysis of cell lysates with commercially available phosphospecific antibodies (fig. S3). These results suggest that the catalytic activity of ZAP-70 plays a role in controlling the basal phosphorylation state of some proteins even in the absence of TCR stimulation. Furthermore, those proteins whose phosphorylation was most substantially changed in the basal state are all implicated in the canonical TCR-stimulated signaling pathway, which suggests that low-level or adapted signaling takes place even without TCR stimulation.

The kinase activity of ZAP-70 affects the phosphorylation of specific regulatory sites on ZAP-70

The Syk family tyrosine kinases Syk and ZAP-70 exhibit a distinct structural organization (*15*, *16*, *45*). N-terminal tandem SH2 domains are connected to the C-terminal kinase domain by a flexible linker. Docking of ZAP-70 to doubly phosphorylated ITAMs involves conformational changes in interdomain A, a segment between the SH2 domains, which facilitates the interactions between interdomain A and the C-lobe of the catalytic domain that contribute to stabilizing the autoinhibitory conformation of the kinase. Release of these interactions promotes the exposure of Tyr^{315} and Tyr^{319} in the linker domain, and the phosphorylation of these residues by Lck further prevents ZAP-70 from returning to the inhibitory conformation (*16*). Moreover, pTyr^{319} serves as a binding site for the SH2 domain of Lck (*16*, *46*–*48*), concentrating activated Lck at the ITAM-bound ZAP-70. These are important regulatory sites that control ZAP-70 function. Transient increases in phosphopeptide abundance for these sites were observed after the inhibition of ZAP-70 kinase activity (Table 1).

In addition, we found a statistically significant increase in the phosphorylation of two tyrosine residues on the kinase domain activation loop of ZAP-70, Tyr^{492} and Tyr^{493}, after 2 min of TCR stimulation, and this difference remained for 10 min after stimulation (Table 1 and Fig. 3), which was validated by Western blotting analysis (fig. S3A). It is well documented that phosphorylation of Tyr^{493} in the activation loop of the kinase domain is required for the full

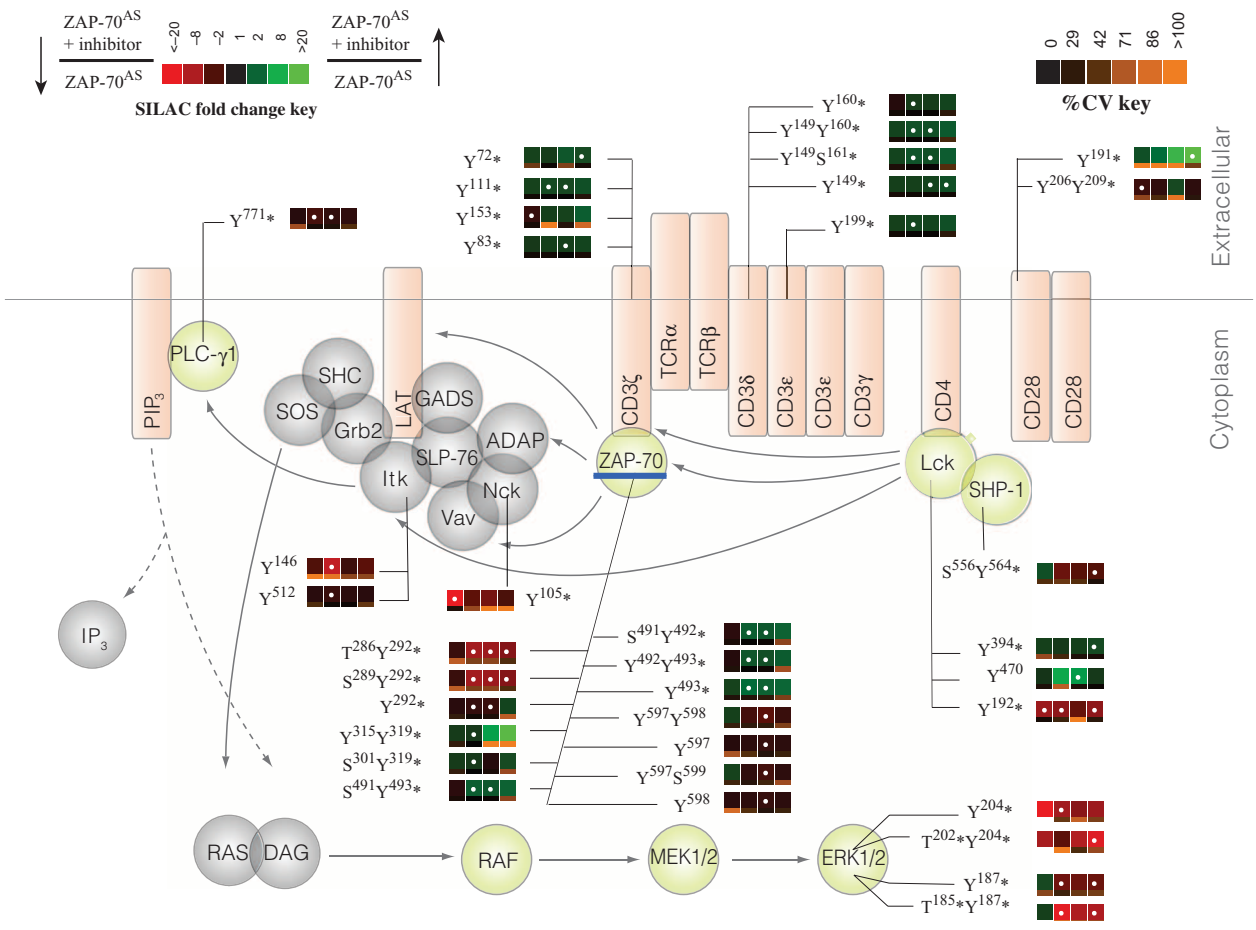

Fig. 3. Targets of ZAP-70–dependent negative feedback regulation in TCR-proximal signaling. A model of the changes in the phosphorylation of TCR signaling components that occurred after inhibition of ZAP-70 catalytic activity (represented by the blue line) illustrated as quantitative SILAC ratio heatmaps beside individual proteins, corresponding to the changes in phosphorylation between the inhibitor-treated and control cells across the four time points of TCR stimulation. Heatmaps were calculated from the average of five independent biological replicate experiments. Green represents increased phosphorylation, whereas red represents decreased phosphorylation in ZAP-70–inhibited cells than in DMSO-treated controls. White dots in the heatmap indicate a statistically significant difference (Q value < 0.05) for that time point and phosphopeptide. Below each heatmap square is a color bar representing the coefficient of variation for that point. Orange represents a high degree of variation, whereas black represents a low degree of variation among the replicate analyses. PIP_3, phosphatidylinositol 3,4,5-trisphosphate; SHC, SH2 domain–containing transforming protein; Grb2, growth factor receptor–bound protein 2; GADS, Grb2-related adaptor downstream of SHC; ADAP, adhesion and degranulation–promoting protein; IP_3, inositol 1,4,5-trisphosphate; MEK1/2, mitogen-activated protein kinase kinase 1 and 2. Asterisk (*) denotes phosphorylation sites previously described in the literature.

catalytic activity of ZAP-70. This site has been described as a substrate for Lck, but it can also serve as a target for ZAP-70 autophosphorylation (*15*). Although Tyr^{492} is also positioned in the activation loop of the kinase domain, its phosphorylation inhibits the catalytic function of ZAP-70 (*11*, *15*, *49*). Because inhibition of ZAP-70 activity led to the increased phosphorylation of Tyr^{493}, our results could reflect the action of a negative feedback mechanism that regulates this site and dampens the activation of ZAP-70. In addition, the data demonstrate that the catalytic activity of ZAP-70 is not an absolute requirement for phosphorylation of Tyr^{493} in cells. Increased Lck activity or increased recruitment of Lck to ZAP-70, which is reflective of the increased phosphorylation of Lck-Tyr^{394}, could account for this phosphorylation.

Several studies suggest that the phosphorylation of ZAP-70 on Tyr^{292} inhibits TCR signaling, possibly through recruitment of the E3 ubiquitin ligase c-Cbl, which dampens TCR activation (*50*–*54*). Inhibition of ZAP-70 kinase activity in our experiments resulted in a marked decrease in the abundance of peptides phosphorylated at this site, with a statistically significant eightfold decrease at 2 to 10 min after TCR stimulation (Table 1 and Fig. 3). This suggests that an early, possibly direct, ZAP-70 kinase–dependent negative regulatory feedback loop dampens ZAP-70 activity by phosphorylating Tyr^{292} after TCR stimulation. Some other previously detected, but less characterized, sites of phosphorylation, such as Tyr^{164} and Tyr^{248}, showed no differences in phosphorylation, whereas the phosphorylation sites Tyr^{597} and Tyr^{598}, which are associated with the full activation of ZAP-70, showed a statistically significant decrease in phosphorylation in response to ZAP-70 inhibition (Table 1).

Together, the changes in the phosphorylation of ZAP-70 that were observed in response to kinase inhibition suggest differential feedback control

of phosphorylation sites on ZAP-70. The kinase activity of ZAP-70 may thus be under the control of feedback mechanisms that control the balance of the phosphorylation of ZAP-70 on sites that could influence activity and subsequent T cell activation. The changes in the phosphorylation of ZAP-70 detected after inhibition of ZAP-70 catalytic activity were mainly seen after TCR engagement and were less evident before TCR stimulation, suggesting that the feedback mechanisms responsible for the regulation of ZAP-70 activity are in place to balance the strength and duration of TCR signaling rather than setting its basal state of activity in resting T cells.

The function of Lck is negatively regulated by ZAP-70 catalytic activity

In resting T cells, a large proportion (~40%) of the kinase Lck exhibits constitutive activation as evidenced by a subset of these Lck molecules that display phosphorylation on Tyr^{394}, the activation loop tyrosine, and a substantial proportion of molecules that are phosphorylated both on the negative regulatory site Tyr^{505} and on Tyr^{394} (*7*). Additional studies support a model whereby ongoing basal signaling tunes the threshold for TCR activation partly through CD45- and Csk-mediated regulation of Lck (*4*, *8*, *9*, *30*, *55*). Our studies enabled us to investigate whether ZAP-70 takes part in the regulation of Lck activity, both in the basal state and after TCR stimulation. As described earlier, we saw a substantial decrease in the phosphorylation of Tyr^{192} in the SH2 domain of Lck after the inhibition of ZAP-70 kinase activity in cells that were not stimulated through the TCR (Fig. 2C). The function of this phosphorylation site is not clear, but it has been implicated in the regulation of Lck (*56*–*58*). Inhibition of ZAP-70 kinase activity also resulted in a statistically significant increase in the phosphorylation of Tyr^{394} on Lck. Dephosphorylation of Lck-Tyr^{394} is dependent, in part, on the phosphatases PTPN22 and SHP-1, whose activities in turn may be dampened by inhibition of the kinase activity of ZAP-70 (*2*, *17*–*19*). Indeed, we saw a substantial decrease in the abundance of the phosphopeptide for SHP-1 Tyr^{564}. Although not as important as $pTyr^{536}$ for SHP-1 activity, $pTyr^{564}$ increases the phosphatase activity of SHP-1 (*17*). In the case of Lck-Tyr^{505}, the peptide that contains this site was identified in this experiment, but it could not be quantified because the tryptic peptide did not contain any arginine or lysine amino acids because it was at the C terminus of the protein.

The SILAC ratios in our experiments also revealed the increased phosphorylation of Lck substrates, such as the TCR ITAMs. The TCR ζ chains contain three ITAMs. The first one includes Tyr^{72} and Tyr^{83}, the second motif contains Tyr^{111} and Tyr^{123}, and the third includes Tyr^{142} and Tyr^{153}. We observed a 1.3-fold increase in the phosphorylation of each of the ITAM tyrosine residues in response to inhibition of ZAP-70 after TCR stimulation (Fig. 2B and table S1). These data provide further evidence that the activity of Lck was increased as a result of inhibition of the catalytic activity of ZAP-70. Similar to the increased phosphorylation of the activation loop of Lck, the increased phosphorylation of the ITAMs was sustained for up to 10 min after TCR stimulation. Additional Lck targets, such as the tyrosine kinase Pyk2, also showed a statistically significant increase (up to 36-fold) in phosphopeptide abundance, both in the basal state and after TCR stimulation (Table 1 and Fig. 3). From these findings, we conclude that the kinase activity of ZAP-70 stimulates a negative feedback loop that inhibits Lck activity and could possibly alter the threshold to subsequent signaling in response to stimuli.

A previous study by one of our groups showed that, in the absence of the ZAP-70 protein (that is, in Jurkat p116 cells), phosphorylation of the N-terminal tyrosine residues of each ITAM in the ζ chain is decreased, whereas phosphorylation of the C-terminal tyrosine residues in each ITAM is increased (*34*). Although the concordant results for the C-terminal tyrosine residues support the idea of a ZAP-70–dependent negative feedback loop that targets the ITAMs, the previous results for the N-terminal tyrosines are discordant with the results obtained with ZAP-70 inhibition in this study. This discrepancy could reflect the absence of the effects of the ZAP-70 tandem SH2 domain in protecting the doubly phosphorylated ITAMs from phosphatases, or it could arise from the order in which the ITAMs are phosphorylated (*59*–*63*).

A computational model suggests a single mechanistic explanation for the data from experiments with ZAP-70 null cells and those from experiments in which ZAP-70 kinase activity was inhibited

Understanding the possible mechanistic origins of the discrepancy between observations made with the $ZAP\text{-}70^{AS}$ system and the ZAP-70 null cells may shed light on how ZAP-70 regulates the earliest events in TCR signaling. To this end, we constructed a number of different computational models and analyzed them to determine whether they could describe our experimental data (see Materials and Methods for computational details). Dissection of these models and associated experiments led us to the model that we propose.

ZAP-70–mediated negative feedback regulation is necessary for concordance with experimental observations

Our computational model of the regulation of TCR signaling by ZAP-70 was based on experimental knowledge gained from previous studies (*14*–*16*, *33*, *64*) and on the results of SILAC experiments with the $ZAP\text{-}70^{AS}$ system and the ZAP-70 null cells. Our model is concerned with inducible signaling. The signal strength is represented by the number of activated Lck molecules at the start of the simulations. Active Lck sequentially phosphorylates each tyrosine residue of the ζ-chain ITAMs, first generating singly phosphorylated ITAMs, which are then converted to doubly phosphorylated motifs (Fig. 4A). In our model, we treat the three ITAM motifs as one because although the contribution of multiple ITAMs will quantitatively amplify signaling (*62*), it is not expected to lead to any qualitative changes. Phosphatases (denoted as "P" in Fig. 4A) dephosphorylate ITAMs to their singly phosphorylated and unphosphorylated states. Next, ZAP-70 is recruited from the cytoplasm to the plasma membrane, and its tandem SH2 domains strongly bind to the doubly phosphorylated ζ-chain ITAMs (Fig. 4B) (*65*, *66*). The binding of ZAP-70 protects the doubly phosphorylated ITAMs from dephosphorylation by phosphatases. Additionally, ZAP-70 can weakly bind head-to-tail with its SH2 domains to singly phosphorylated sites of the N- and C-terminal phosphotyrosines of each ζ-chain ITAM (*66*); that is, the C-terminal SH2 domain of ZAP-70 weakly binds to the N-terminal tyrosine residue of ITAMs (Fig. 4B) and vice versa (*33*, *67*, *68*).

Once ZAP-70 is bound to the doubly phosphorylated ζ-chain ITAMs, active Lck phosphorylates tyrosine residues Tyr^{315} and Tyr^{319} in the SH2-kinase linker domain of ZAP-70 to generate a conformationally open ZAP-70. The subsequent phosphorylation of Tyr^{493} in the catalytic domain of ZAP-70 promotes its full activation (Fig. 4C). ZAP-70 can be dephosphorylated by phosphatases (denoted by "P_z" in Fig. 4C) to form its inactive states. The model for inhibitor-treated cells expressing $ZAP\text{-}70^{AS}$ (denoted $ZAP\text{-}70^{AS}$ + inhibitor cells) excludes the last ZAP-70 phosphorylation step, which converts ZAP-70 from the open to the active state, because the inhibitor blocks the kinase activity of $ZAP\text{-}70^{AS}$.

The $ZAP\text{-}70^{AS}$ SILAC experiments suggested a possible ZAP-70 kinase activity–dependent negative feedback loop that could regulate the phosphorylation of ζ-chain ITAMs. Thus, we included ZAP-70–mediated negative feedback regulation into the models for all of the cell types, except for the ZAP-70 null cells (Fig. 4C). In the model, both open and

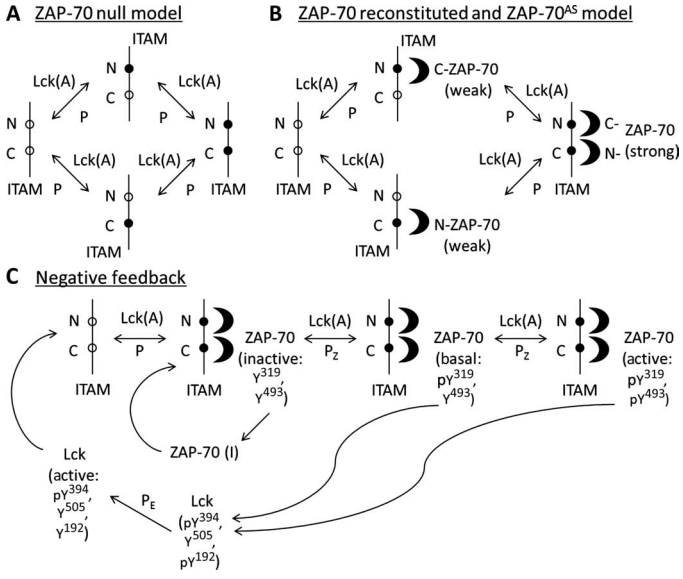

Fig. 4. Computational model of proximal TCR signaling. (A) In ZAP-70 null cells, active Lck [Lck(A)] sequentially phosphorylates [whereas phosphatases (P) dephosphorylate] the N- and C-terminal tyrosines in individual ITAMs, generating singly phosphorylated and later doubly phosphorylated ITAMs. (B) In the ZAP-70 reconstituted cells or in ZAP-70AS cells, ZAP-70 weakly binds to the singly phosphorylated ITAMs and strongly binds to the doubly phosphorylated ITAMs. (C) Active Lck phosphorylates the SH2-linker tyrosine residues Y^{315} and Y^{319} of ZAP-70, generating open ZAP-70. The subsequent phosphorylation by Lck of Y^{493} generates active ZAP-70. Active and open forms of ZAP-70 are dephosphorylated by phosphatases (P_Z). Active and open forms of ZAP-70 phosphorylate a negative regulatory site (Y^{192}) in Lck. The phosphatases denoted by "P_E" dephosphorylate Lck to return it to its active state. Active Lck further regulates ITAM phosphorylation through this negative feedback loop.

active forms of ZAP-70 phosphorylate the negative regulatory site Tyr^{192} in Lck, thus generating an inactive Lck state (Fig. 4C). The model would perform identically if any other ZAP-70–mediated negative feedback loop affected Lck. The ZAP-70–mediated negative feedback regulation competes with the protective effect of ZAP-70 on ITAM phosphorylation.

The calculated ZAP-70 null/ZAP-70 reconstituted SILAC ratio (that is, the ratio of the relative abundance of a detected phosphopeptide in ZAP-70 null cells to that in the cells reconstituted with ZAP-70) decreased at early times and increased at later time points for the N- and C-terminal ζ-chain ITAMs (Fig. 5A, "ZAP-70 NF"), which is consistent with the trend suggested by experimental results for the C-terminal, but not the N-terminal, tyrosines in the ITAMs. The ZAP-70 null/ZAP-70 reconstituted SILAC ratio decreased at early times because the negative feedback loop is downstream of the binding of ZAP-70 to the ITAMs; thus, at early times, the protective function of ZAP-70 is dominant, whereas at later times, this situation reverses because, in our model, the protective function of ZAP-70 on ITAM phosphorylation (because of its binding) is weaker than the negative feedback loop that ZAP-70 mediates. If parameters were chosen to reverse this, the SILAC ratio would decrease at all times (Fig. 5A, "ZAP-70 bind") for both the N- and C-terminal tyrosines. The results of our calculations with this model showed that the ZAP-70AS + inhibitor/ZAP-70AS SILAC ratio increased for the N- and C-terminal tyrosines of ζ-chain ITAMs over time (Fig. 5B, "ZAP-70 NF"), which was consistent with the experimental data. This is a direct result of the inhibition of upstream events by ZAP-70 introduced into the model, without which this SILAC ratio would decrease because the protective function of ZAP-70 would dominate (Fig. 5B, "ZAP-70 bind"). Comparison between the experimental observations and this model suggests that substantial ZAP-70 kinase activity–mediated inhibition is necessary and sufficient to describe most of the data, but this model fails to capture the asymmetry between the behavior of the N- and C-terminal ITAM tyrosines for the ZAP-70 null/ZAP-70 reconstituted SILAC ratio that is suggested by the experimental data.

Models that describe the asymmetry in ITAM phosphorylation make predictions for experimental tests

Studies of T and B cells report that Src family kinases may initially phosphorylate the N-terminal tyrosines and then phosphorylate the C-terminal tyrosines of each ITAM (*61*, *69*). We added to the model described earlier the possibility that Lck affects fast initial phosphorylation of the N-terminal tyrosines (compared to the C-terminal ones) in each ζ-chain ITAM. This is followed by the binding of Lck to the phosphorylated tyrosine and then the phosphorylation of the adjacent tyrosine by Lck (Fig. 6A). Once a doubly phosphorylated ITAM is produced, the binding of ZAP-70 to it is strongly preferred compared to the binding of Lck.

The results of our calculations with this model showed that the ZAP-70 null/ZAP-70 reconstituted SILAC ratio decreased at early times and ultimately approached unity for the N-terminal tyrosine residues. This ratio decreased at early times and increased for the C-terminal tyrosine residues in each ITAM (Fig. 5A, "ITAM and Lck"). The binding of ZAP-70 to phosphorylated ITAMs prevents the action of phosphatases. The decrease in the ratio at the early time points was a result of the loss of the protective function of ZAP-70 on ITAM phosphorylation. At later times, the absence of the negative feedback loop in ZAP-70 null cells was dominant for the C-terminal ITAM tyrosines; however, for the N-terminal tyrosines, in the absence of ZAP-70, Lck could still bind to this phosphorylated tyrosine and protect it from dephosphorylation. Thus, the absence of the negative feedback loop was compensated for by the fast rate of phosphorylation of the N-terminal tyrosine and the binding of Lck to it. This made the SILAC ratio approach unity. The results of this model are consistent with experimental data for the ZAP-70AS + inhibitor/ZAP-70AS SILAC ratio because it increased for N- and C-terminal tyrosines in ζ-chain ITAMs over time (Fig. 5B, "ITAM and Lck").

These calculated results require that the Lck SH2 domain bind to the singly phosphorylated ITAMs with high affinity, which is comparable to the binding affinity of ZAP-70 for the doubly phosphorylated ITAMs, which was possibly facilitated by the plasma membrane environment (see the Supplementary Materials). Once bound, Lck would rapidly phosphorylate neighboring tyrosine residues in each ITAM with faster kinetics than that of the initial ITAM phosphorylation events. This is because strongly bound Lck has a higher effective concentration for the phosphorylation of neighboring tyrosines (see the Supplementary Materials). The fast second phosphorylation is necessary to efficiently create doubly phosphorylated ITAMs that can bind to ZAP-70 to activate the negative feedback loop, thus promoting negative feedback regulation. The fast phosphorylation of the N-terminal tyrosine and the binding of Lck to it would mediate the protective function for this tyrosine that was noted earlier.

To test whether Lck bound strongly to singly phosphorylated ITAM tyrosines, we performed experiments to measure these quantities in solution (see the Supplementary Materials). Consistent with past experiments (*66*), we found that the binding affinity of the Lck SH2 domain for singly phosphorylated N- and C-terminal ITAMs was in the micromolar range (fig. S4 and table S4). To obtain good correlation with the SILAC data, however, we required a higher binding affinity in the model. This iteration

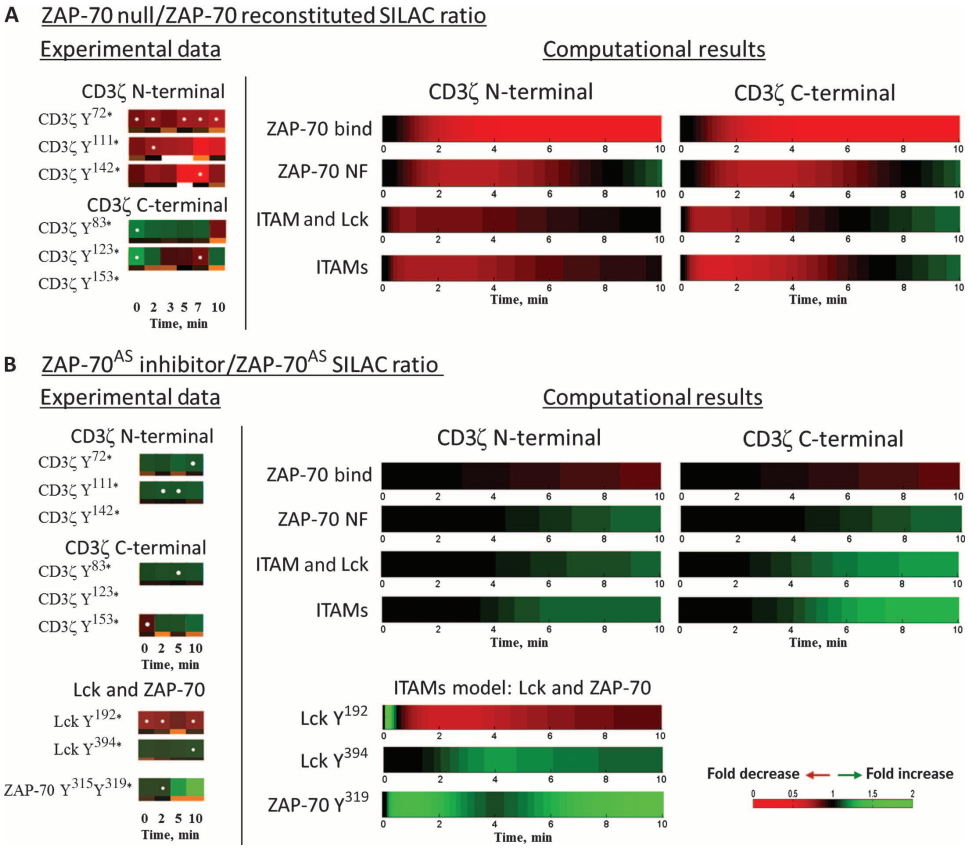

Fig. 5. Correlation between the experimental and calculated SILAC ratios. (A) Comparison of the experimental (left) and calculated (right) SILAC ratios of the N- and C-terminal tyrosines in each ITAM for the ZAP-70 null/ZAP-70 reconstituted system as a ratio heatmap. (B) Comparison of the experimental (left) and calculated (right) SILAC ratios for tyrosine phosphorylation of ζ-chain ITAMs, Lck, and ZAP-70 proteins of the ZAP-70AS + inhibitor/ZAP-70AS system as a ratio heatmap. The experimental ZAP-70 null/ZAP-70 reconstituted SILAC ratios (left panel) were taken from a previous study (*34*). The calculated SILAC ratios (right) were determined for the presence of various biological effects. The "ZAP-70 bind" model captures the results when ZAP-70–mediated negative feedback is absent. The "ZAP-70 NF" model shows the results when ZAP-70–medited negative feedback occurs. The "ITAM and Lck" model illustrates the results with the fast initial phosphorylation of the N-terminal tyrosine residues of ITAMs by Lck and the subsequent binding of the SH2 domain of Lck to the N- and C-terminal tyrosines. The "ITAMs" model captures the results with ordered phosphorylation of ζ-chain ITAM tyrosines (scenarios 1, 2, and 3). The "ITAM and Lck" and "ITAMs" models include the ZAP-70–mediated negative feedback. The calculated SILAC ratios for the tyrosine phosphorylation of the Lck and ZAP-70 proteins of the ZAP-70AS + inhibitor/ZAP-70AS system are shown only for the ITAMs model. In the heatmap, red indicates a decrease in phosphorylation, black indicates no change, and green represents an increase in phosphorylation when comparing ZAP-70 null cells to ZAP-70 reconstituted cells or ZAP-70AS inhibited cells versus DMSO-treated control cells. The experimental phosphorylation of Y^{153} in the ZAP-70 null/ZAP-70 reconstituted SILAC ratio and of Y^{142} and Y^{123} in the ZAP-70AS + inhibitor/ZAP-70AS SILAC ratio were not detected, which is indicated by missing heatmaps. Asterisk (*) denotes phosphorylation sites previously described in the literature.

between the SILAC data, computational modeling, and experiments led us to abandon this model and search for alternative explanations involving Lck.

Extensive parameter sensitivity studies suggested that a few scenarios pertaining to the Lck-mediated phosphorylation of N- and C-terminal ITAM tyrosines could explain the asymmetry in phosphorylation suggested by the SILAC data on ZAP-70 null and reconstituted cells. The four steps of ITAM phosphorylation are characterized by reaction rate constants: k_1, k_2, k_3, and k_4 (Fig. 6B). We found that three combinations of the relative values of these rate constants were consistent with the experimental data. (i) $k_2 > k_1 = k_3 = k_4$: the C-terminal tyrosine is singly phosphorylated much faster than are all of the other tyrosine residues. (ii) $k_2 = k_3 > k_1 = k_4$: phosphorylation of the C-terminal tyrosine is faster than that of the N-terminal tyrosine, regardless of whether singly or doubly phosphorylated ITAMs are produced. (iii) $k_1 = k_3 > k_2 = k_4$: phosphorylaton of the first tyrosine is faster than that of the N-terminal tyrosine, which is followed by rapid phosphorylation of the C-terminal residue without the need for Lck to be bound to the phosphorylated N-terminal tyrosine of the ITAM.

For each of these situations, we found that the ZAP-70 null/ZAP-70 reconstituted SILAC ratio for the N-terminal tyrosine approached unity at later times, whereas that for the C-terminal tyrosine increased (Fig. 5, "ITAMs"). In the first two cases, this is because the number of ITAMs with singly phosphorylated C-terminal tyrosines exceeded the number of ITAMs with singly phosphorylated N-terminal tyrosines. The ZAP-70–mediated negative feedback loop acted on both singly and doubly phosphorylated ITAMs, but the protective effect of ZAP-70 on phosphorylated states acted only on doubly phosphorylated ITAMs. Because there were more singly phosphorylated C-terminal tyrosines, the absence of ZAP-70–mediated negative feedback resulted in an increase in the phosphorylation of C-terminal tyrosines. For the N-terminal tyrosines, negative feedback and the protective effect of ZAP-70 were approximately equivalent. In the third scenario, because k_1 and k_3 are both large (compared to the rates of action of phosphatases), the number of ITAMs with singly phosphorylated N-terminal tyrosines was determined by a balance between the production of singly phosphorylated ITAMs and their subsequent double phosphorylation. The concentration of active Lck appeared in precisely the same functional form in the rates of occurrence of both of these steps. ZAP-70–mediated negative feedback reduced the concentration of active Lck; however, because the concentration of active Lck appears in the expression for the rates of single phosphorylation and subsequent double phosphorylation in exactly the same way, the number of singly phosphorylated N-terminal tyrosines does not substantially change much upon removal of ZAP-70.

Our systematic dissection of various models led to the following mechanistic picture that yields results consistent with the two independent sets of SILAC experiments. The model includes ZAP-70–mediated negative feedback regulation of Lck activity and three different possibilities for the relative rates of phosphorylation of the N- and C-terminal ITAM tyrosines by Lck. We must note that although our model focused on Lck, we

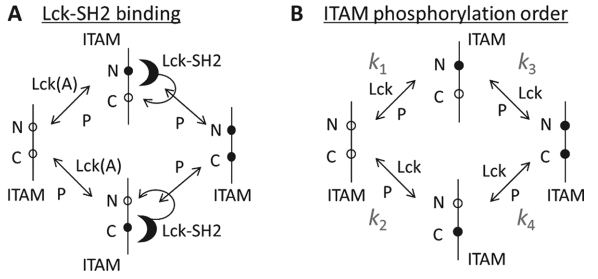

Fig. 6. Computational models that describe the asymmetry in ITAM phosphorylation. (A) Active Lck sequentially phosphorylates [and the phosphatases (P) dephosphorylate] the N- and C-terminal tyrosines in each ITAM, generating singly phosphorylated and later doubly phosphorylated ITAMs. Next, Lck binds through its noncatalytic SH2 domain to the phosphorylated N- and C-terminal tyrosines of each ITAM. Once bound, Lck rapidly phosphorylates the neighboring C- and N-terminal tyrosines of each ITAM, generating doubly phosphorylated ITAMs. (B) Kinetic scheme of the order of tyrosine phosphorylation in ITAMs according to scenarios 1, 2, and 3. k_1 and k_2 are the rates of production of singly phosphorylated N- and C-terminal tyrosines from their unphosphorylated forms, respectively, whereas k_3 and k_4 are the rates of production of doubly phosphorylated N- and C-terminal tyrosines from their singly phosphorylated forms, respectively.

cannot exclude the possibility that other proteins with SH2 domains (or phosphotyrosine-binding domains) or phosphatases have preference for the N-terminal versus the C-terminal tyrosines and could account for the observed asymmetry of ITAM phosphorylation.

DISCUSSION

Our understanding of what determines TCR signaling threshold and strength is still limited, and the regulatory mechanisms of proximal TCR signaling in resting T cells, as well as after TCR engagement, need to be further characterized. By undertaking both quantitative mass spectrometry experiments and computational modeling, we have studied the role of ZAP-70 in the regulation of initial TCR signaling events. On the basis of our results, we suggest that the catalytic activity of ZAP-70, in addition to its vital role for downstream TCR signaling that leads to cellular responses, also promotes negative feedback mechanisms that target Lck and its substrates, as well as ZAP-70 itself. Our studies reveal a role for ZAP-70–dependent negative feedback in the regulation of the basal state, as well as after TCR stimulation.

The activity of ZAP-70 orchestrates signaling downstream of the TCR, including phosphorylation of the adaptor proteins LAT and SLP-76 and the assembly of intracellular signaling complexes. Deficiency of either SLP-76 or LAT results in phosphorylation changes that, in part, resemble those that we detected after inhibition of ZAP-70 catalytic activity, resulting in increased phosphorylation of upstream signaling molecules, such as Lck (Tyr^{394}), and of some of the TCR ITAM tyrosines at early time points after TCR ligation (*39*, *40*). In addition, Jurkat T cells lacking SLP-76 or LAT exhibit increased phosphorylation of the activating site Tyr^{493} of ZAP-70, which is potentially a result of the increased activity of Lck or ZAP-70. One possible interpretation of these findings is that the ZAP-70–dependent negative regulatory effects observed in our study may be the result of an indirect mechanism that requires the presence of LAT and SLP-76, as well as further downstream players, such as the phosphatases SHP-1 or CD45, to target Lck, its substrates, or both. This does not necessarily exclude a direct ZAP-70–mediated effect on Lck, such as its phosphorylation of Lck. Indeed, both our modeling data and mass spectrometry data suggest such a mechanism. TCR ligation leads to alterations in the phosphorylation of Lck, including phosphorylation of Tyr^{192} at the end of the β strand E in the SH2 domain of Lck, which can be mediated by Syk family kinases. Phosphorylation of this site prevents the binding of the Lck SH2 domain to Lck substrates and correlates with reduced signaling downstream of the TCR (*56*–*58*), thus representing a plausible mechanism for ZAP-70–mediated negative feedback on Lck.

Unlike previous studies with cells containing fixed genetic lesions, our methodology using rapid inhibition of ZAP-70 before TCR stimulation enabled us to also detect perturbation of basal signaling and to study ZAP-70–dependent feedback at play even in the absence of TCR ligation. Even in the basal state, we saw a marked decrease in the phosphorylation of Lck Tyr^{192}, which suggests that a potential ZAP-70–dependent feedback mechanism involving this site occurs also in resting cells before TCR stimulation occurs.

SILAC experiments with ZAP-70 null cells suggested an asymmetry in the phosphorylation of N- and C-terminal tyrosine residues in each of the ζ-chain ITAMs (Fig. 5). Our modeling reproduced this ITAM asymmetry by invoking a role for ordered phosphorylation of ITAM tyrosines (Fig. 5, "ITAMs"). Several studies showed that Lck initially phosphorylates the N-terminal tyrosine of ITAMs and then later phosphorylates the C-terminal tyrosine (*61*, *69*); however, the precise order of ITAM phosphorylation is still under investigation (*60*, *61*, *63*, *69*). In the computational part of our study that focused on Lck, we found three possible scenarios for ordered ITAM phosphorylation that were consistent with the SILAC data (Fig. 5, "ITAMs"). In one scenario, Lck phosphorylates the C-terminal tyrosine faster than it phosphorylates the N-terminal tyrosine in the production of singly phosphorylated ITAMs, whereas in another scenario, Lck phosphorylates the C-terminal tyrosine faster in the production of singly and doubly phosphorylated ITAMs. The third possibility is that once Lck initially phosphorylates the N-terminal tyrosine in ITAMs, the rate of phosphorylation of the neighboring ITAM C-terminal tyrosine must be faster or equivalent to that of the initial tyrosine.

These scenarios describe the simplest kinase specificity model that could account for the observed asymmetry in the phosphorylation of ITAMs. However, one can speculate that the ordered dephosphorylation of ITAMs by tyrosine phosphatases or the asymmetric binding preference of single SH2 domain– or phosphotyrosine binding domain (PTB)–containing proteins for singly phosphorylated ITAM phosphorylation sites could also reproduce the observed asymmetry. Experimental tests of some of these possibilities would require evaluation of kinetic catalytic rate parameters of Lck for the N- and C-terminal tyrosines at the membrane, preferably in cells, which would be challenging. Moreover, in cells, other proteins could also affect the phosphorylation of these sites. Identifying ITAM phosphatases that might have preference for the N-terminal versus the C-terminal site and, as mentioned earlier, other proteins with SH2 domains that could bind to these sites, for example, the adaptor protein Shc (*70*), is beyond the scope of the present study.

Alternatively, the results of our modeling showed that the asymmetry in ITAM tyrosine phosphorylation could also be reproduced if there is preferential binding of the SH2 domain of Lck to the singly phosphorylated N-terminal tyrosine in ITAMs and the subsequent processive phosphorylation of C-terminal tyrosines by Lck, similar to observations in B cells (*71*). However, this assumption is discordant with the experimentally measured binding affinities of the Lck SH2 domain for singly phosphorylated ITAMs (fig. S4 and table S4) (*66*). One possibility to consider is that the kinetic parameters measured in solution do not reflect what happens at the membrane, where there could be increased Lck binding kinetics because of the reduced dimensionality (*72*, *73*) and a higher effective local concentration of Lck (described in the Supplementary Materials). One

other possible consideration is that clustered phosphorylated ITAMs may activate Lck by kinase dimerization, leading to the trans-phosphorylation of Lck (*71*). A final possibility is that the binding of the Lck SH2 domain stabilizes the open, active conformation of Lck, leading to increased kinase activity and thus increased phosphorylation of ITAMs (*71*). To evaluate these possibilities further, additional experimental testing of our models will be required.

Strict but dynamic control of the catalytic activities of both Lck and ZAP-70 in T cells is necessary to facilitate rapid, adequate responses to pathogens and transformed cells while at the same time providing sufficient dampening of perturbations to ensure self-tolerance. Reciprocal regulation of Lck and ZAP-70 may provide an additional line of control for the basal steady state, which is poised for activation by TCR agonists. Expression of hypomorphic mutant alleles of ZAP-70 can cause reactivity to self-ligands and autoimmune disease (*74*–*77*). Loss of proper negative regulation of proximal TCR signaling could contribute to such immunological disorders. Our results stress the role of ZAP-70 as a key regulator of T cell activation, and further clarification of the mechanism behind the negative feedback loops dependent on ZAP-70 should provide insights into the mechanisms controlling T cell function in the basal state, how thresholds for responsiveness are established, and how TCR-dependent signaling is calibrated.

MATERIALS AND METHODS

Cell culture, SILAC labeling, and T cell stimulation

The human T cell leukemic line Jurkat p116 stably expressing ZAP-70AS was previously described (*35*). SILAC labeling was performed as previously described (*34*). Briefly, cells in logarithmic growth phase were washed twice and then maintained in RPMI-1640 without arginine and lysine (Pierce Biotechnology) containing either "light" $^{12}C_6$, $^{14}N_4$ arginine and $^{12}C_6$, $^{14}N_2$ lysine (Sigma) or "heavy" $^{13}C_6$, $^{15}N_4$ arginine and $^{13}C_6$, $^{15}N_2$ lysine (Cambridge Isotope Laboratories), supplemented with 10% dialyzed fetal calf serum (Invitrogen) at 37°C and 5% CO_2 for seven doublings. The concentrations of lysine and arginine used for SILAC labeling were 0.22 and 0.38 mM, respectively. For stimulation, cells were harvested and reconstituted in phosphate-buffered saline at 1×10^8 cell/ml and were rested for 30 min at 37°C. Before stimulation, SILAC heavy–labeled cells were treated with 10 μM HXJ-42 (the ZAP-70AS inhibitor) for 1.5 min (*36*), whereas SILAC light–labeled cells were treated with DMSO as a vehicle control for the same time. For TCR stimulation, for each time point, 1×10^8 cells were treated with OKT3 and OKT4 antibodies (2.5 μg/ml each; eBioscience), which are specific for CD3 and CD4, respectively, for 30 s at 37 °C. Cross-linking antibody IgG (22 μg/ml; Jackson ImmunoResearch) was then added, and cells were incubated for 0, 2, 5, or 10 min. Stimulation was halted by incubation of the cells in lysis buffer [9 M urea, 1 mM sodium orthovanadate, 20 mM Hepes, 2.5 mM sodium pyrophosphate, and 1 mM β-glycerophosphate (pH 8.0)] for 20 min at 4°C. Lysates were then sonicated at a 30-W output with two bursts of 30 s each and then were cleared by centrifugation at 20,000*g* for 15 min at 4°C. Quantitative phosphoproteomic mass spectral analysis was performed using a modified phosphotyrosine peptide immunoprecipitation protocol (*41*) as described in detail in the Supplementary Materials.

Computational modeling

We constructed several theoretical models of upstream T cell signaling pathways and simulated them by solving the ordinary differential equations with the Matlab SimBiology software (*78*). Our biochemical models (including kinases and phosphatases) are well mixed and use mass action kinetic laws to describe protein-protein interactions and enzymatic activities. The signaling model details and the parameters used in the simulations are noted in the Supplementary Materials. We also performed sensitivity analysis for the parameters for which no experimental information was available (see the Supplementary Materials). We conducted a few calculations incorporating stochastic effects and found that the mechanistic conclusions we reached from the deterministic analyses remained unchanged.

SUPPLEMENTARY MATERIALS

www.sciencesignaling.org/cgi/content/full/8/377/ra49/DC1

Experimental procedures.

Computational modeling.

Fig. S1. Reproducibility of proteomic quantitative data in the absence of TCR stimulation.

Fig. S2. Reproducibility of proteomic quantitative data for all TCR stimulation time points.

Fig. S3. Validation of inhibitor specificity.

Fig. S4. Binding of the SH2 domain of Lck to monophosphorylated TCR ζ-chain ITAM peptides.

Fig. S5. The number of rebinding events between enzymes and substrates upon variation of different kinetic parameters.

Fig. S6. Description of the ZAP-70 allosteric model and the results of calculations with this model.

Fig. S7. Sensitivity analysis of the kinetic parameters used in calculations for the "ITAM and Lck" model.

Fig. S8. Sensitivity analysis of the kinetic parameters used in calculations for the "ITAMs" model.

Fig. S9. Sensitivity analysis of the kinetic parameters used in calculations for the ZAP-70 allosteric model (part I).

Fig. S10. Sensitivity analysis of the kinetic parameters used in calculations for the ZAP-70 allosteric model (part II).

Table S1. Complete list of sequence and phosphorylation site assignments of all identified phosphopeptides with corresponding SIC peak areas and statistics, protein association numbers, gene ontology, and KEGG functional annotation.

Table S2. Complete list of phosphopeptides detected from every replicate and time point of TCR stimulation.

Table S3. Fold change between HXJ-42–treated and DMSO-treated ZAP-70AS cells and *Q* values for peptides listed in Table 1.

Table S4. Binding parameters for the Lck SH2 domain and monophosphorylated ζ ITAM peptides determined by isothermal titration calorimetry at 25°C.

Table S5. Concentrations of species used in calculations for all models (volume = 1 μm^3).

Table S6. Reactions and kinetic parameters used in calculations for the ZAP-70–mediated negative feedback model and models used to reproduce an asymmetry in ITAM phosphorylation.

Table S7. Reactions and kinetic parameters used in calculations for the ZAP-70 allosteric function model.

Table S8. Sensitivity analysis of the concentrations of signaling molecules used in calculations for the "ITAM and Lck" and "ITAMs" models.

Table S9. Sensitivity analysis of the kinetic parameters used in calculations for the "ITAM and Lck" model.

Table S10. Sensitivity analysis of the kinetic parameters used in calculations for the "ITAMs" model.

Table S11. Sensitivity analysis of the concentrations of signaling molecules used in calculations for the ZAP-70 allosteric model.

Table S12. Sensitivity analysis of the kinetic parameters used in calculations for ZAP-70 allosteric model.

References (*79*–*94*)

REFERENCES AND NOTES

1. J. E. Smith-Garvin, G. A. Koretzky, M. S. Jordan, T cell activation. *Annu. Rev. Immunol.* **27**, 591–619 (2009).
2. R. J. Brownlie, R. Zamoyska, T cell receptor signalling networks: Branched, diversified and bounded. *Nat. Rev. Immunol.* **13**, 257–269 (2013).
3. M. S. Jordan, A. L. Singer, G. A. Koretzky, Adaptors as central mediators of signal transduction in immune cells. *Nat. Immunol.* **4**, 110–116 (2003).
4. Y. X. Tan, J. Zikherman, A. Weiss, Novel tools to dissect the dynamic regulation of TCR signaling by the kinase Csk and the phosphatase CD45. *Cold Spring Harb. Symp. Quant. Biol.* 131–139 (2013).
5. L. M. Chow, M. Fournel, D. Davidson, A. Veillette, Negative regulation of T-cell receptor signalling by tyrosine protein kinase p50^{csk}. *Nature* **365**, 156–160 (1993).
6. M. L. Hermiston, J. Zikherman, J. W. Zhu, CD45, CD148, and Lyp/Pep: Critical phosphatases regulating Src family kinase signaling networks in immune cells. *Immunol. Rev.* **228**, 288–311 (2009).

7. K. Nika, C. Soldani, M. Salek, W. Paster, A. Gray, R. Etzensperger, L. Fugger, P. Polzella, V. Cerundolo, O. Dushek, T. Höfer, A. Viola, O. Acuto, Constitutively active Lck kinase in T cells drives antigen receptor signal transduction. *Immunity* **32**, 766–777 (2010).
8. J. Zikherman, C. Jenne, S. Watson, K. Doan, W. Raschke, C. C. Goodnow, A. Weiss, CD45-Csk phosphatase-kinase titration uncouples basal and inducible T cell receptor signaling during thymic development. *Immunity* **32**, 342–354 (2010).
9. J. R. Schoenborn, Y. X. Tan, C. Zhang, K. M. Shokat, A. Weiss, Feedback circuits monitor and adjust basal Lck-dependent events in T cell receptor signaling. *Sci. Signal.* **4**, ra59 (2011).
10. S. E. Ziemba, S. L. Menard, M. J. McCabe, A. J. Rosenspire, T-cell receptor signaling is mediated by transient Lck activity, which is inhibited by inorganic mercury. *FASEB J.* **23**, 1663–1671 (2009).
11. J. D. Watts, J. S. Sanghera, S. L. Pelech, R. Aebersold, Phosphorylation of serine 59 of $p56^{lck}$ in activated T cells. *J. Biol. Chem.* **268**, 23275–23282 (1993).
12. D. G. Winkler, I. Park, T. Kim, N. S. Payne, C. T. Walsh, J. L. Strominger, J. Shin, Phosphorylation of Ser-42 and Ser-59 in the N-terminal region of the tyrosine kinase $p56^{lck}$. *Proc. Natl. Acad. Sci. U.S.A.* **90**, 5176–5180 (1993).
13. T. Brdicka, T. A. Kadlecek, J. P. Roose, A. W. Pastuszak, A. Weiss, Intramolecular regulatory switch in ZAP-70: Analogy with receptor tyrosine kinases. *Mol. Cell. Biol.* **25**, 4924–4933(2005).
14. S. Deindl, T. A. Kadlecek, T. Brdicka, X. Cao, A. Weiss, J. Kuriyan, Structural basis for the inhibition of tyrosine kinase activity of ZAP-70. *Cell* **129**, 735–746 (2007).
15. H. Wang, T. A. Kadlecek, B. B. Au-Yeung, H. E. S. Goodfellow, L. Y. Hsu, T. S. Freedman, A. Weiss, ZAP-70: An essential kinase in T-cell signaling. *Cold Spring Harb. Perspect. Biol.* **2**, a002279 (2010).
16. Q. Yan, T. Barros, P. R. Visperas, S. Deindl, T. A. Kadlecek, A. Weiss, J. Kuriyan, Structural basis for activation of ZAP-70 by phosphorylation of the SH2-kinase linker. *Mol. Cell. Biol.* **33**, 2188–2201 (2013).
17. U. Lorenz, SHP-1 and SHP-2 in T cells: Two phosphatases functioning at many levels. *Immunol. Rev.* **228**, 342–359 (2009).
18. O. Acuto, V. Di Bartolo, F. Michel, Tailoring T-cell receptor signals by proximal negative feedback mechanisms. *Nat. Rev. Immunol.* **8**, 699–712 (2008).
19. I. Štefanová, B. Hemmer, M. Vergelli, R. Martin, W. E. Biddison, R. N. Germain, TCR ligand discrimination is enforced by competing ERK positive and SHP-1 negative feedback pathways. *Nat. Immunol.* **4**, 248–254 (2003).
20. F. Huang, H. Gu, Negative regulation of lymphocyte development and function by the Cbl family of proteins. *Immunol. Rev.* **224**, 229–238 (2008).
21. S. J. F. Cronin, J. M. Penninger, From T-cell activation signals to signaling control of anti-cancer immunity. *Immunol. Rev.* **220**, 151–168 (2007).
22. R. Mashima, Y. Hishida, T. Tezuka, Y. Yamanashi, The roles of Dok family adapters in immunoreceptor signaling. *Immunol. Rev.* **232**, 273–285 (2009).
23. V. Horejsí, Transmembrane adaptor proteins in membrane microdomains: Important regulators of immunoreceptor signaling. *Immunol. Lett.* **92**, 43–49 (2004).
24. K.-H. Lee, A. R. Dinner, C. Tu, G. Campi, S. Raychaudhuri, R. Varma, T. N. Sims, W. R. Burack, H. Wu, J. Wang, O. Kanagawa, M. Markiewicz, P. M. Allen, M. L. Dustin, A. K. Chakraborty, A. S. Shaw, The immunological synapse balances T cell receptor signaling and degradation. *Science* **302**, 1218–1222 (2003).
25. Q.-J. Li, A. R. Dinner, S. Qi, D. J. Irvine, J. B. Huppa, M. M. Davis, A. K. Chakraborty, CD4 enhances T cell sensitivity to antigen by coordinating Lck accumulation at the immunological synapse. *Nat. Immunol.* **5**, 791–799 (2004).
26. M. L. Dustin, A. K. Chakraborty, A. S. Shaw, Understanding the structure and function of the immunological synapse. *Cold Spring Harb. Perspect. Biol.* **2**, a002311 (2010).
27. T. Yokosuka, K. Sakata-Sogawa, W. Kobayashi, M. Hiroshima, A. Hashimoto-Tane, M. Tokunaga, M. L. Dustin, T. Saito, Newly generated T cell receptor microclusters initiate and sustain T cell activation by recruitment of Zap70 and SLP-76. *Nat. Immunol.* **6**, 1253–1262 (2005).
28. O. Dushek, J. Goyette, P. A. van der Merwe, Non-catalytic tyrosine-phosphorylated receptors. *Immunol. Rev.* **250**, 258–276 (2012).
29. E. Markegard, E. Trager, C. O. Yang, W. Zhang, A. Weiss, J. P. Roose, Basal LAT-diacylglycerol-RasGRP1 signals in T cells maintain TCRα gene expression. *PLOS One* **6**, e25540 (2011).
30. Y. X. Tan, B. N. Manz, T. S. Freedman, C. Zhang, K. M. Shokat, A. Weiss, Inhibition of the kinase Csk in thymocytes reveals a requirement for actin remodeling in the initiation of full TCR signaling. *Nat. Immunol.* **15**, 186–194 (2014).
31. J. N. Mandl, J. P. Monteiro, N. Vrisekoop, R. N. Germain, T cell-positive selection uses self-ligand binding strength to optimize repertoire recognition of foreign antigens. *Immunity* **38**, 263–274 (2013).
32. N. Manjarrez-Orduño, E. Marasco, S. A. Chung, M. S. Katz, J. F. Kiridly, K. R. Simpfendorfer, J. Freudenberg, D. H. Ballard, E. Nashi, T. J. Hopkins, D. S. Cunninghame Graham, A. T. Lee, M. J. H. Coenen, B. Franke, D. W. Swinkels, R. R. Graham, R. P. Kimberly, P. M. Gaffney, T. J. Vyse, T. W. Behrens, L. A. Criswell, B. Diamond, P. K. Gregersen, CSK regulatory polymorphism is associated with systemic lupus erythematosus and influences B-cell signaling and activation. *Nat. Genet.* **44**, 1227–1230 (2012).
33. B. B. Au-Yeung, S. Deindl, L.-Y. Hsu, E. H. Palacios, S. E. Levin, J. Kuriyan, A. Weiss, The structure, regulation, and function of ZAP-70. *Immunol. Rev.* **228**, 41–57 (2009).
34. V. Nguyen, L. Cao, J. T. Lin, N. Hung, A. Ritz, K. Yu, R. Jianu, S. P. Ulin, B. J. Raphael, D. H. Laidlaw, L. Brossay, A. R. Salomon, A new approach for quantitative phosphoproteomic dissection of signaling pathways applied to T cell receptor activation. *Mol. Cell. Proteomics* **8**, 2418–2431 (2009).
35. S. E. Levin, C. Zhang, T. A. Kadlecek, K. M. Shokat, A. Weiss, Inhibition of ZAP-70 kinase activity via an analog-sensitive allele blocks T cell receptor and CD28 superagonist signaling. *J. Biol. Chem.* **283**, 15419–15430 (2008).
36. B. B. Au-Yeung, H. J. Melichar, J. O. Ross, D. A. Cheng, J. Zikherman, K. M. Shokat, E. A. Robey, A. Weiss, Quantitative and temporal requirements revealed for Zap70 catalytic activity during T cell development. *Nat. Immunol.* **15**, 687–694 (2014).
37. B. B. Au-Yeung, J. Zikherman, J. L. Mueller, J. F. Ashouri, M. Matloubian, D. A. Cheng, Y. Chen, K. M. Shokat, A. Weiss, A sharp T-cell antigen receptor signaling threshold for T-cell proliferation. *Proc. Natl. Acad. Sci. U.S.A.* **111**, E3679–E3688 (2014).
38. B. B. Au-Yeung, S. E. Levin, C. Zhang, L.-Y. Hsu, D. A. Cheng, N. Killeen, K. M. Shokat, A. Weiss, A genetically selective inhibitor demonstrates a function for the kinase Zap70 in regulatory T cells independent of its catalytic activity. *Nat. Immunol.* **11**, 1085–1092 (2010).
39. M. Salek, S. McGowan, D. C. Trudgian, O. Dushek, B. de Wet, G. Efstathiou, O. Acuto, Quantitative phosphoproteome analysis unveils LAT as a modulator of CD3ζ and ZAP-70 tyrosine phosphorylation. *PLOS One* **8**, e77423 (2013).
40. L. Cao, Y. Ding, N. Hung, K. Yu, A. Ritz, B. J. Raphael, A. R. Salomon, Quantitative phosphoproteomics reveals SLP-76 dependent regulation of PAG and Src family kinases in T cells. *PLOS One* **7**, e46725 (2012).
41. Y. A. Helou, V. Nguyen, S. P. Beik, A. R. Salomon, ERK positive feedback regulates a widespread network of tyrosine phosphorylation sites across canonical T cell signaling and actin cytoskeletal proteins in Jurkat T cells. *PLOS One* **8**, e69641 (2013).
42. J. D. Storey, A direct approach to false discovery rates. *J. R. Stat. Soc. Series B Stat. Methodol.* **64**, 479–498 (2002).
43. J. D. Storey, The positive false discovery rate: A Bayesian interpretation and the q-value. *Ann. Stat.* **31**, 2013–2035 (2003).
44. J. D. Storey, R. Tibshirani, Statistical significance for genomewide studies. *Proc. Natl. Acad. Sci. U.S.A.* **100**, 9440–9445 (2003).
45. U. Grädler, D. Schwarz, V. Dresing, D. Musil, J. Bomke, M. Frech, H. Greiner, S. Jäkel, T. Rysiok, D. Müller-Pompalla, A. Wegener, Structural and biophysical characterization of the Syk activation switch. *J. Mol. Biol.* **425**, 309–333 (2013).
46. M. Pelosi, Tyrosine 319 in the interdomain B of ZAP-70 is a binding site for the Src homology 2 domain of Lck. *J. Biol. Chem.* **274**, 14229–14237 (1999).
47. Q. Zhao, B. L. Williams, R. T. Abraham, A. Weiss, Interdomain B in ZAP-70 regulates but is not required for ZAP-70 signaling function in lymphocytes. *Mol. Cell. Biol.* **19**, 948–956 (1999).
48. B. L. Williams, B. J. Irvin, S. L. Sutor, C. C. Chini, E. Yacyshyn, J. Bubeck Wardenburg, M. Dalton, A. C. Chan, R. T. Abraham, Phosphorylation of Tyr319 in ZAP-70 is required for T-cell antigen receptor-dependent phospholipase C-γ1 and Ras activation. *EMBO J.* **18**, 1832–1844 (1999).
49. A. C. Chan, M. Dalton, R. Johnson, G. H. Kong, T. Wang, R. Thoma, T. Kurosaki, Activation of ZAP-70 kinase activity by phosphorylation of tyrosine 493 is required for lymphocyte antigen receptor function. *EMBO J.* **14**, 2499–2508 (1995).
50. Q. Zhao, A. Weiss, Enhancement of lymphocyte responsiveness by a gain-of-function mutation of ZAP-70. *Mol. Cell. Biol.* **16**, 6765–6774 (1996).
51. M. L. Lupher Jr., K. A. Reedquist, S. Miyake, W. Y. Langdon, H. Band, A novel phosphotyrosine-binding domain in the N-terminal transforming region of Cbl interacts directly and selectively with ZAP-70 in T cells. *J. Biol. Chem.* **271**, 24063–24068 (1996).
52. M. L. Lupher Jr., Z. Songyang, S. E. Shoelson, L. C. Cantley, H. Band, The Cbl phosphotyrosine-binding domain selects a D(N/D)XpY motif and binds to the Tyr^{292} negative regulatory phosphorylation site of ZAP-70. *J. Biol. Chem.* **272**, 33140–33144 (1997).
53. N. Rao, M. L. Lupher, S. Ota, K. A. Reedquist, B. J. Druker, H. Band, The linker phosphorylation site Tyr^{292} mediates the negative regulatory effect of Cbl on ZAP-70 in T cells. *J. Immunol.* **164**, 4616–4626 (2000).
54. A. Magnan, V. Di Bartolo, A.-M. Mura, C. Boyer, M. Richelme, Y.-L. Lin, A. Roure, A. Gillet, C. Arrieumerlou, O. Acuto, B. Malissen, M. Malissen, T cell development and T cell responses in mice with mutations affecting tyrosines 292 or 315 of the Zap-70 protein tyrosine kinase. *J. Exp. Med.* **194**, 491–505 (2001).
55. L. McNeill, R. J. Salmond, J. C. Cooper, C. K. Carret, R. L. Cassady-Cain, M. Roche-Molina, P. Tandon, N. Holmes, D. R. Alexander, The differential regulation of Lck kinase phosphorylation sites by CD45 is critical for T cell receptor signaling responses. *Immunity* **27**, 425–437 (2007).
56. C. Couture, Z. Songyang, T. Jascur, S. Williams, P. Tailor, L. C. Cantley, T. Mustelin, Regulation of the Lck SH2 domain by tyrosine phosphorylation. *J. Biol. Chem.* **271**, 24880–24884 (1996).
57. C. Couture, G. Baier, C. Oetken, S. Williams, D. Telford, A. Marie-Cardine, G. Baier-Bitterlich, S. Fischer, P. Burn, A. Altman, Activation of $p56^{lck}$ by $p72^{syk}$ through physical association and N-terminal tyrosine phosphorylation. *Mol. Cell. Biol.* **14**, 5249–5258 (1994).

58. M. Soula, B. Rothhut, L. Camoin, J. L. Guillaume, D. Strosberg, T. Vorherr, P. Burn, F. Meggio, S. Fischer, R. Fagard, Anti-CD3 and phorbol ester induce distinct phosphorylated sites in the SH2 domain of $p56^{lck}$. *J. Biol. Chem.* **268**, 27420–27427 (1993).
59. E. N. Kersh, A. S. Shaw, P. M. Allen, Fidelity of T cell activation through multistep T cell receptor ζ phosphorylation. *Science* **281**, 572–575 (1998).
60. N. S. van Oers, B. Tohlen, B. Malissen, C. R. Moomaw, S. Afendis, C. A. Slaughter, The 21- and 23-kD forms of TCRζ are generated by specific ITAM phosphorylations. *Nat. Immunol.* **1**, 322–328 (2000).
61. H. R. Housden, P. J. S. Skipp, M. P. Crump, R. J. Broadbridge, T. Crabbe, M. J. Perry, M. G. Gore, Investigation of the kinetics and order of tyrosine phosphorylation in the T-cell receptor ζ chain by the protein tyrosine kinase Lck. *Eur. J. Biochem.* **270**, 2369–2376 (2003).
62. H. Mukhopadhyay, S.-P. Cordoba, P. K. Maini, P. A. van der Merwe, O. Dushek, Systems model of T Cell receptor proximal signaling reveals emergent ultrasensitivity. *PLOS Comput. Biol.* **9**, e1003004 (2013).
63. P. E. Love, S. M. Hayes, ITAM-mediated signaling by the T-cell antigen receptor. *Cold Spring Harb. Perspect. Biol.* **2**, a002485 (2010).
64. A. Weiss, T cell antigen receptor signal transduction: A tale of tails and cytoplasmic protein-tyrosine kinases. *Cell* **73**, 209–212 (1993).
65. S. Deindl, T. A. Kadlecek, X. Cao, J. Kuriyan, A. Weiss, Stability of an autoinhibitory interface in the structure of the tyrosine kinase ZAP-70 impacts T cell receptor response. *Proc. Natl. Acad. Sci. U.S.A.* **106**, 20699–20704 (2009).
66. M. E. Labadia, R. H. Ingraham, J. Schembri-King, M. M. Morelock, S. Jakes, Binding affinities of the SH2 domains of ZAP-70, p^{56}*lck* and *Shc* to the ζ chain ITAMs of the T-cell receptor determined by surface plasmon resonance. *J. Leukoc. Biol.* **59**, 740–746 (1996).
67. M. H. Hatada, X. Lu, E. R. Laird, J. Green, J. P. Morgenstern, M. Lou, C. S. Marr, T. B. Phillips, M. K. Ram, K. Theriault, Molecular basis for interaction of the protein tyrosine kinase ZAP-70 with the T-cell receptor. *Nature* **377**, 32–38 (1995).
68. K. Fütterer, J. Wong, R. A. Grucza, A. C. Chan, G. Waksman, Structural basis for Syk tyrosine kinase ubiquity in signal transduction pathways revealed by the crystal structure of its regulatory SH2 domains bound to a dually phosphorylated ITAM peptide. *J. Mol. Biol.* **281**, 523–537 (1998).
69. L. I. Pao, S. J. Famiglietti, J. C. Cambier, Asymmetrical phosphorylation and function of immunoreceptor tyrosine-based activation motif tyrosines in B cell antigen receptor signal transduction. *J. Immunol.* **160**, 3305–3314 (1998).
70. K. S. Ravichandran, K. K. Lee, Z. Songyang, L. C. Cantley, P. Burn, S. J. Burakoff, Interaction of Shc with the ζ chain of the T cell receptor upon T cell activation. *Science* **262**, 902–905 (1993).
71. S. A. Johnson, C. M. Pleiman, L. Pao, J. Schneringer, K. Hippen, J. C. Cambier, Phosphorylated immunoreceptor signaling motifs (ITAMs) exhibit unique abilities to bind and activate Lyn and Syk tyrosine kinases. *J. Immunol.* **155**, 4596–4603 (1995).
72. S. M. Abel, J. P. Roose, J. T. Groves, A. Weiss, A. K. Chakraborty, The membrane environment can promote or suppress bistability in cell signaling networks. *J. Phys. Chem. B* **116**, 3630–3640 (2012).
73. E. Hui, R. D. Vale, In vitro membrane reconstitution of the T-cell receptor proximal signaling network. *Nat. Struct. Mol. Biol.* **21**, 133–142 (2014).
74. N. Sakaguchi, T. Takahashi, H. Hata, T. Nomura, T. Tagami, S. Yamazaki, T. Sakihama, T. Matsutani, I. Negishi, S. Nakatsuru, S. Sakaguchi, Altered thymic T-cell selection due to a mutation of the ZAP-70 gene causes autoimmune arthritis in mice. *Nature* **426**, 454–460 (2003).
75. S. Sakaguchi, N. Sakaguchi, H. Yoshitomi, H. Hata, T. Takahashi, T. Nomura, Spontaneous development of autoimmune arthritis due to genetic anomaly of T cell signal transduction: Part 1. *Semin. Immunol.* **18**, 199–206 (2006).
76. O. M. Siggs, L. A. Miosge, A. L. Yates, E. M. Kucharska, D. Sheahan, T. Brdicka, A. Weiss, A. Liston, C. C. Goodnow, Opposing functions of the T cell receptor kinase ZAP-70 in immunity and tolerance differentially titrate in response to nucleotide substitutions. *Immunity* **27**, 912–926 (2007).
77. L.-Y. Hsu, Y. X. Tan, Z. Xiao, M. Malissen, A. Weiss, A hypomorphic allele of ZAP-70 reveals a distinct thymic threshold for autoimmune disease versus autoimmune reactivity. *J. Exp. Med.* **206**, 2527–2541 (2009).
78. *Matlab and SimBiology Toolbox* (The MathWorks Inc., Natick, MA, 2012); http://www.mathworks.com/products/simbiology/.
79. J. Rappsilber, Y. Ishihama, M. Mann, Stop and go extraction tips for matrix-assisted laser desorption/ionization, nanoelectrospray, and LC/MS sample pretreatment in proteomics. *Anal. Chem.* **75**, 663–670 (2003).
80. K. Yu, A. R. Salomon, PeptideDepot: Flexible relational database for visual analysis of quantitative proteomic data and integration of existing protein information. *Proteomics* **9**, 5350–5358 (2009).
81. K. Yu, A. R. Salomon, HTAPP: High-throughput autonomous proteomic pipeline. *Proteomics* **10**, 2113–2122 (2010).
82. S. B. Ficarro, A. R. Salomon, L. M. Brill, D. E. Mason, M. Stettler-Gill, A. Brock, E. C. Peters, Automated immobilized metal affinity chromatography/nano-liquid chromatography/electrospray ionization mass spectrometry platform for profiling protein phosphorylation sites. *Rapid Commun. Mass Spectrom.* **19**, 57–71 (2005).
83. D. N. Perkins, D. J. Pappin, D. M. Creasy, J. S. Cottrell, Probability-based protein identification by searching sequence databases using mass spectrometry data. *Electrophoresis* **20**, 3551–3567 (1999).
84. K. Yu, A. Sabelli, L. DeKeukelaere, R. Park, S. Sindi, C. A. Gatsonis, A. Salomon, Integrated platform for manual and high-throughput statistical validation of tandem mass spectra. *Proteomics* **9**, 3115–3125 (2009).
85. J. E. Elias, S. P. Gygi, Target-decoy search strategy for increased confidence in large-scale protein identifications by mass spectrometry. *Nat. Methods* **4**, 207–214 (2007).
86. S. A. Beausoleil, J. Villén, S. A. Gerber, J. Rush, S. P. Gygi, A probability-based approach for high-throughput protein phosphorylation analysis and site localization. *Nat. Biotechnol.* **24**, 1285–1292 (2006).
87. H. Edelhoch, Spectroscopic determination of tryptophan and tyrosine in proteins. *Biochemistry* **6**, 1948–1954 (1967).
88. N. J. Anthis, G. M. Clore, Sequence-specific determination of protein and peptide concentrations by absorbance at 205 nm. *Protein Sci.* **22**, 851–858 (2013).
89. M. R. Clark, S. A. Johnson, J. C. Cambier, Analysis of Ig-α–tyrosine kinase interaction reveals two levels of binding specificity and tyrosine phosphorylated Ig-α stimulation of Fyn activity. *EMBO J.* **13**, 1911–1919 (1994).
90. G. I. Bell, Models for the specific adhesion of cells to cells. *Science* **200**, 618–627 (1978).
91. C. C. Govern, M. K. Paczosa, A. K. Chakraborty, E. S. Huseby, Fast on-rates allow short dwell time ligands to activate T cells. *Proc. Natl. Acad. Sci. U.S.A.* **107**, 8724–8729 (2010).
92. M. N. Artyomov, M. Lis, S. Devadas, M. M. Davis, A. K. Chakraborty, CD4 and CD8 binding to MHC molecules primarily acts to enhance Lck delivery. *Proc. Natl. Acad. Sci. U.S.A.* **107**, 16916–16921 (2010).
93. S. Mukherjee, J. Zhu, J. Zikherman, R. Parameswaran, T. A. Kadlecek, Q. Wang, B. Au-Yeung, H. Ploegh, J. Kuriyan, J. Das, A. Weiss, Monovalent and multivalent ligation of the B cell receptor exhibit differential dependence upon Syk and Src family kinases. *Sci. Signal.* **6**, ra1 (2013).
94. E. Tsang, A. M. Giannetti, D. Shaw, M. Dinh, J. K. Y. Tse, S. Gandhi, H. Ho, S. Wang, E. Papp, J. M. Bradshaw, Molecular mechanism of the Syk activation switch. *J. Biol. Chem.* **283**, 32650–32659 (2008).

Acknowledgments: We thank B. Au-Yeung and M. Mollenauer from the Weiss laboratory for excellent experimental advice and technical support. **Funding:** This work was supported in part by NIH grants P01 AI91580 and R01 AI083636; Wenner-Gren Foundations, Sweden (to H.S.-G.); Stiftelsen Blanceflor Boncompagni Ludovisi, född Bildt (to H.S.-G.); Sweden-America Foundation (to H.S.-G.); and Cancer Research Institute Irvington Fellowship (to M.P.F.). **Author contributions:** M.P.F., A.K.C., and A.W. designed the computational research; M.P.F. performed simulations and mathematical calculations; M.P.F., A.K.C., and A.W. analyzed the data and wrote parts of the paper; H.S.-G., Q.J., T.A.K., D.A.C., A.J.C., and J.K. designed and performed the experiments and wrote parts of the paper; and A.R.S., A.K.C., and A.W. conceived of the work, wrote the paper, and supervised the work. **Competing interests:** The authors declare that they have no competing interests. **Data and materials availability:** The mass spectrometry proteomics data have been deposited to the ProteomeXchange Consortium through the PRIDE partner repository with the data set identifier PXD002023.

Submitted 16 June 2014
Accepted 30 April 2015
Final Publication 19 May 2015
10.1126/scisignal.2005596
Citation: H. Sjölin-Goodfellow, M. P. Frushicheva, Q. Ji, D. A. Cheng, T. A. Kadlecek, A. J. Cantor, J. Kuriyan, A. K. Chakraborty, A. R. Salomon, A. Weiss, The catalytic activity of the kinase ZAP-70 mediates basal signaling and negative feedback of the T cell receptor pathway. *Sci. Signal.* **8**, ra49 (2015).

The catalytic activity of the kinase ZAP-70 mediates basal signaling and negative feedback of the T cell receptor pathway

Hanna Sjölin-Goodfellow, Maria P. Frushicheva, Qinqin Ji, Debra A. Cheng, Theresa A. Kadlecek, Aaron J. Cantor, John Kuriyan, Arup K. Chakraborty, Arthur R. Salomon and Arthur Weiss (May 19, 2015)

Science Signaling **8** (377), ra49. [doi: 10.1126/scisignal.2005596]